

Resolving Estuarine Nitrogen Use by Phytoplankton Communities Using a Whole Ecosystem Tracer Approach

Jaylyn W. Babitch 1,2 • James A. Nelson 1 • Linda A. Deegan 3 • Hillary Sullivan 3,4 • Beth A. Stauffer 1

Received: 6 May 2020 / Revised: 29 December 2020 / Accepted: 18 January 2021 © Coastal and Estuarine Research Federation 2021

Abstract

The use of nutrients by diverse phytoplankton communities in estuarine systems, and their response to changes in physical and biogeochemical processes in these natural systems, is a significant ongoing area of research. We used a whole ecosystem $^{15}NO_3^-$ tracer experiment to determine the uptake of different nitrogen (N) forms in phytoplankton functional groups over a mid-to neap tidal cycle in a salt marsh creek in Plum Island Estuary, Massachusetts, USA. We quantified the biomass and $\delta^{15}N$ for three groups corresponding to micro- (20–200 μ m; microP), nano- (3–20 μ m; nanoP), and picophytoplankton (< 3 μ m; picoP). All three size classes showed distinct use of recycled N sources throughout the 11-day sampling period and minimal direct assimilation of the $^{15}NO_3^-$ tracer. MicroP consistently used high amounts of creek-derived $^{15}NH_4^+$, even with a shift at neap tide from diatom- to dinoflagellate-dominated communities (including members of the harmful genus *Alexandrium*). NanoP use of recycled $^{15}NH_4^+$ increased over the mid-neap tidal cycle, while picoP use decreased. Both biomass and NH_4^+ use (as highest $\delta^{15}N$ values) of all size groups were maximized during neap tide. This study demonstrates partitioning of recycled N use among size-based phytoplankton groups in the estuary, with distinct effects of tidal cycle on the nutrient uptake of each group, and with important implications for the roles of diverse phytoplankton communities in estuarine nutrient cycling.

Keywords Phytoplankton · Functional groups · Tidal forcing · ¹⁵N · Stable isotopes

Communicated by Hans W. Paerl

> Jaylyn W. Babitch jaylyn.babitch@sanjoseca.gov

James A. Nelson nelson@louisiana.edu

Linda A. Deegan ldeegan@woodwellclimate.org

Hillary Sullivan hsullivan@woodwellclimate.org

Published online: 18 February 2021

- Department of Biology, University of Louisiana at Lafayette, Lafayette, LA, USA
- Present address: Environmental Services Department, City of San José, San Jose, CA, USA
- Woodwell Climate Research Center, Falmouth, MA, USA
- Marine Science Center, Northeastern University, Nahant, MA, USA

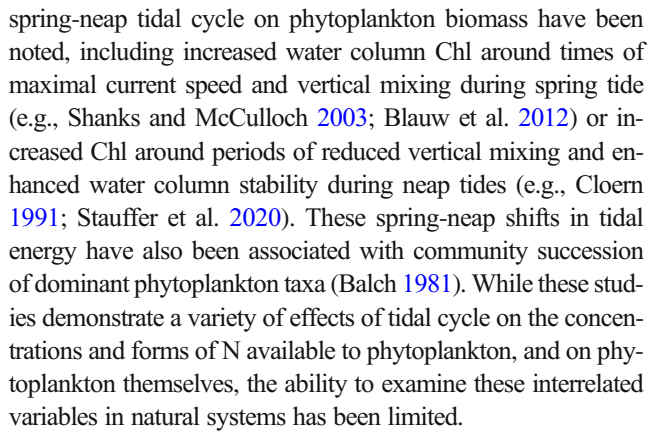
Introduction

Estuarine ecosystems are characterized by significant temporal and spatial variability in the physical and biogeochemical processes that affect phytoplankton distribution and growth (Vallino and Hopkinson 1998; Cloern et al. 2014). Tidal forcing causes physical mixing and advection, which drive changes in phytoplankton biomass and composition, nutrient cycling, and food web transfer over the flood-ebb (Wetz et al. 2006; Leles et al. 2014) and spring-neap tidal cycles (Balch 1981; Shanks and McCulloch 2003; Stauffer et al. 2020). However, the effects of tidally-mediated nutrient and biomass dynamics on diverse communities of phytoplankton require further investigation. Such investigations are especially necessary given the ability of different phytoplankton groups to uniquely respond to changes in both physical forcing and the concentrations and forms of nitrogen (N) that are available (Margalef 1978; Glibert 2016; Moschonas et al. 2017) and which contribute to coastal eutrophication and harmful algal blooms (HABs; e.g., Howarth et al. 1996; Rabalais 2002).



Various phytoplankton functional groups and species preferentially use different forms of dissolved N, including nitrate (NO₃⁻), ammonium (NH₄⁺), and dissolved organic N (DON; e.g., Glibert et al. 2016). Several studies have found that smaller phytoplankton generally take up higher proportions of reduced N forms (NH₄⁺ and DON) than larger phytoplankton (e.g., Probyn et al. 1990; Maguer et al. 2009; Glibert et al. 2016) and that DON, alone, can support phytoplankton production throughout the year (Moschonas et al. 2017). Bronk et al. (2007) showed that NO₃ supports the growth of larger taxa, such as diatoms, increasing the amount of high-nutrient food available for zooplankton, while NH₄⁺ and DON decrease food web efficiency by promoting the growth of smaller groups, such as cyanobacteria that are generally less nutritious to grazers. Moschonas et al. (2017) also showed that reduced or organic forms of N strongly contributed to N uptake in small (< 10 µm) phytoplankton throughout the year in a Scottish fjord. In contrast, bottle bioassays performed by Koch and Gobler (2009) found that enrichment with reduced N forms stimulated the growth of larger (> 5 μ m) diatoms and dinoflagellates in Long Island, New York estuaries. It is also well-documented that forms of N interact with each other. Specifically, high concentrations of NH₄⁺ relative to NO₃⁻ can suppress phytoplankton NO₃ uptake (e.g., Carpenter and Dunham 1985; Dortch 1990; Dugdale et al. 2007) and/ or increase toxin production by HAB dinoflagellates in the genus Alexandrium (Leong et al. 2004; Hattenrath et al. 2010). DON can also be an important nutrient for a variety of HAB species (as reviewed in Davidson et al. 2012). Taken as a whole, this rich literature suggests highly variable N use by different phytoplankton groups, including HABs, in bottle bioassay experiments conducted throughout estuarine and coastal ecosystems.

Such complex biogeochemical interactions are further complicated by estuarine or coastal hydrodynamics, including tidal forcing, which control physical mixing, advection, and biogeochemistry across multiple spatiotemporal scales in these systems but are not incorporated into typical bottle or microcosm-based experiments. Diurnal and biweekly tidal cycles impact both concentrations and forms of N that are available, as well as the biomass and community composition of phytoplankton in estuaries. The diurnal flood-ebb tidal cycle can facilitate seeping of microbially-remineralized N from sediment porewater into the water column in marsh creeks (Koch and Gobler 2009; Spivak and Ossolinski 2016), providing a source of recycled N forms for estuarine phytoplankton. Changes in total chlorophyll a (Chl; Wetz et al. 2006) and abundance of specific taxa (e.g., pennate diatoms; Leles et al. 2014) have also been observed over flood-ebb tidal cycles in estuaries. Spring tides that flood marsh platforms result in lower water column dissolved inorganic N (DIN) concentrations, relative to neap tides, in marsh tidal creeks in macrotidal estuarine environments (e.g., Vörösmarty and Loder III 1994). A number of effects of the



The current study seeks to investigate how phytoplankton groups use different forms of N in a tidally-driven estuarine ecosystem. Using a whole system ¹⁵N tracer approach in a salt marsh tidal creek (Holmes et al. 2000; Hughes et al. 2000; Tobias et al. 2003a), we quantified the relative uptake of N by size-based functional groups of phytoplankton over the mid to neap and flood-ebb time scales of the tidal cycle. Advantages of this approach over bottle-based experiments include incorporating the effects of natural environmental conditions (including physical drivers) on nutrient and phytoplankton dynamics (Tobias et al. 2003a) and avoiding effects associated with enclosure in bottles on both biomass and community composition of microbes (Zobell 1943; Holmboe et al. 1999). Previous in situ tracer studies have addressed only whole phytoplankton biomass (Tobias et al. 2003a; Deegan et al. 2007; York et al. 2007; Drake et al. 2009; Duernberger et al. 2011), only microphytoplankton (> 20 µm; Holmes et al. 2000), or only a few specific taxa (Hughes et al. 2000). The current study resolves phytoplankton groups, including those < 20 µm in size which play different roles in food webs and nutrient cycling than larger sizes, while also resolving biomass and major taxonomic groups in the larger size classes. By elucidating the N cycling functions of distinct phytoplankton groups in a tidally varying salt marsh ecosystem, we can better understand how tidally-driven changes in nutrients and phytoplankton communities may impact recycling and fate of N, composition and quality of primary production, and nutrient transfer through the estuarine food web.

Methods

Experimental Design

The stable isotope tracer addition experiment was conducted over a mid-neap tidal cycle from 10 to 19 July 2016 (Julian day 192–201), in a primary tidal creek in Plum Island Estuary (PIE), Massachusetts, USA (Fig. 1). "Mid" is defined as middle of the transition from spring to neap, i.e., the study commenced several days following the spring tide. Additional



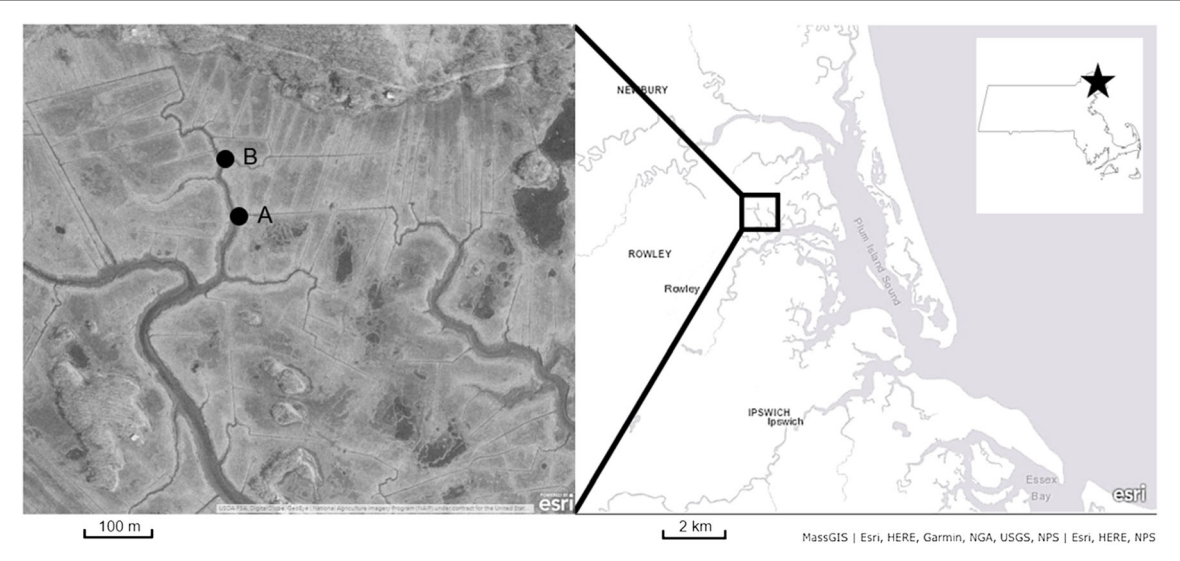


Fig. 1 Left: aerial image of the study site at West Creek, Plum Island Estuary, with black dots indicating the ¹⁵N addition site (A; 42.739° N, 70.848° W) and sampling site (B; 42.740° N, 70.848° W). Right: map of

Plum Island Sound, with black rectangle showing the study site and inset showing its location (star) within Massachusetts, USA

samples were collected on 20 July 2016 (Julian day 202), following the end of tracer addition. PIE is a macrotidal New England estuary, typical of the region, that experiences semidiurnal tides. PIE is the site of long-term monitoring and experimental research on estuarine ecosystem function (Plum Island Ecosystems Long Term Ecological Research (PIE LTER); pie-lter.ecosystems.mbl.edu 2018). The study site was located at West Creek in the Rowley River watershed of PIE (39 km²; Fig. 1), which serves as an unmodified reference site for a long-term N enrichment experiment as part of the TIDE project (Deegan et al. 2007). West Creek is in the middle salt marsh area of PIE, which has an average tidal range of 2.6 m (Spivak and Ossolinski 2016). A band of tall Spartina alterniflora (TSA) along the creek edge is flooded to a depth of approximately 10 cm during mid tides, while the entire marsh platform can be flooded during spring tides. During neap tides, water fills the creek channel but does not flood the TSA. The study period encompassed transitions from TSA-flooding mid tide (days 192–195) to creek-flooding neap tide (days 196-201), and back to mid tide (day 202). These periods are referred to as "TSA" versus "creek" flooding throughout the rest of this paper.

We used a whole ecosystem ¹⁵NO₃⁻ tracer addition into West Creek to track the relative N uptake of different ecosystem members using methods consistent with previous PIE tracer experiments (Holmes et al. 2000; Tobias et al. 2003a; Drake et al. 2009) and briefly summarized below. The ¹⁵N addition pump was located at 42.74° N, 70.85° W in West Creek, and the sampling site was located approximately 80 m landward/upstream of the addition site (Fig. 1). The sampling location was chosen because it represented where the water column became well mixed, and it left approximately 200 m of the creek upstream for N processing and removal. A 10 g

L⁻¹ solution of 10% K¹⁵NO₃ was added into the surface water at the pump site during flood tides beginning at 23:00 on day 191 and ending at 12:00 on day 201. The molar mass of total NO₃⁻ added represented < 1% of natural NO₃⁻ in flooding waters. The pump was turned on when the water level of a flood tide reached 0.2 m above a sensor positioned at the creek bottom (Onset water level logger), and it was shut off at the start of ebb tide, a threshold defined as two consecutive negative changes in water height (measured every 10 min). The solution addition rate (155–500 mL min⁻¹) was adjusted every 10 min based on a water flux calibration curve, derived from the relationship between water level and discharge, to maintain a consistent concentration in the water flowing past the addition site and to reach a target $\delta^{15}N$ of 3000 % at the sampling site. Therefore, any changes in water column δ^{15} N upstream of the addition site could be attributed to N transformation and removal processes.

Water Column Nutrients and Hydrodynamics

Over the 10-day tracer addition, surface water samples for analysis of $\mathrm{NO_3}^-$ and $\delta^{15}\mathrm{NO_3}^-$, $\mathrm{NH_4}^+$ and $\delta^{15}\mathrm{NH_4}^+$, $\mathrm{PO_4}^{3-}$, and total suspended solids (TSS) were collected once per day at the addition and sampling sites during daylight hours and within 2 h of high tide. Additional samples were collected every 3–4 h over five diurnal cycles during TSA flooding (days 193, 194, and 202) and creek flooding periods (days 196 and 198). These samples were collected at timepoints corresponding with flood, high, and ebb points in the diurnal tidal cycle. Nutrient and TSS samples were filtered through pre-combusted GF/F filters and frozen until analysis at PIE. Concentrations of $\mathrm{PO_4}^{3-}$ and $\mathrm{NO_3}^{-}$ were analyzed using colorimetry on an autoanalyzer (Lachat Instruments) following standard methods (Johnson and Petty



1982, 1983). Concentrations of NH_4^+ were analyzed spectrophotometrically using the indophenol method (Schneider 1976). Water column dissolved $\delta^{15}NO_3^-$ and $\delta^{15}NH_4^+$ were measured using modified ammonia diffusion methods (Sigman et al. 1997; Holmes et al. 1998).

Water height and surface current speed were measured at the addition site every 10 min with an Acoustic Doppler Current Profiler (ADCP; Teledyne Streampro2). Water height at the sampling site was calculated using the average difference in water level logger measurements between the sites of addition and sampling (0.2 m). Dissolved oxygen concentration (DO), temperature, and salinity were measured every 5 min throughout the experiment using a multiparameter sonde (YSI EXO2) positioned at the creek bottom approximately 20 m landward of the addition site.

Phytoplankton Sample Collection and Analysis

Water samples for phytoplankton were collected at the same time as the nutrient samples, within 2 h of high tide every day and every 3-4 h over five diurnal cycles, as described above. For each sampling timepoint, 8 L of water was collected from the surface in acid-washed (5% HCl) and DI water rinsed polycarbonate bottles. Bottles were transported back to the lab at PIE and kept protected from light. Within 1-3 h, whole seawater (WSW) from each sample was sequentially filtered through 200 μ m Nitex mesh (< 200 μ m), 20- μ m Nitex mesh (< 20 μ m), and 3 µm membrane filters (Whatman Nuclepore track etch; < 3 µm). Approximately 100–200 mL of filtrate from each size fraction was gently vacuum-filtered onto duplicate 25-mm glass fiber filters (Whatman GF/F), which were then stored in plastic tissue processing capsules at − 20 °C until analysis. Filters were analyzed for Chl biomass by fluorescence (Turner Designs 10AU), with overnight extraction in 90% acetone and acid-correction for phaeopigments (Strickland and Parsons 1972). To calculate microphytoplankton (microP, $20-200 \mu m$) biomass, the < $20-\mu m$ Chl measurements were subtracted from the < 200-µm Chl measurements. To calculate nanophytoplankton (nanoP, 3–20 μm) biomass, the < 3-μm Chl measurements were subtracted from the < 20-µm Chl measurements. The < 3-µm Chl measurements directly represented picophytoplankton (picoP, < 3 μm) biomass.

Additional water (generally 300–400 mL) from each size-fractionated sample was vacuum-filtered onto duplicate, precombusted (4 h at 500 °C), 25 mm GF/F filters. These filters were placed in plastic Petri dishes and stored at $-20\,^{\circ}\text{C}$. Samples were then dried at 50 °C for 48 h and analyzed for ^{15}N on a Europa ANCA-SL elemental analyzer gas chromatograph preparation system attached to a continuous-flow Europa 20-20 gas source stable isotope ratio-mass spectrometer (IR-MS) at the Marine Biological Laboratory (Woods Hole, Massachusetts). The $\delta^{15}\text{N}$ of each filter was determined by standard calculations (Peterson and Fry 1987). These filter

 $\delta^{15}N$ measurements and the biomass proportions of each phytoplankton size class on the filters (as determined by Chl measurements) were used to calculate size-specific $\delta^{15}N$. PicoP $\delta^{15}N$ was equal to $\delta^{15}N$ measured on the < 3-µm filters. NanoP $\delta^{15}N$ was calculated as:

$$\delta^{15}N_{nano} = \left(\delta^{15}N_{20} - \left(\delta^{15}N_{pico} \times F_{pico20}\right)\right) / F_{nano20}$$

where $\delta^{15}N_{20}$ is $\delta^{15}N$ measured on the < 20- μ m filters, $\delta^{15}N_{pico}$ is picoP $\delta^{15}N$, F_{nano20} is the fraction of nanoP Chl on the < 20- μ m filters, and F_{pico20} is the fraction of picoP Chl on the < 20- μ m filters. MicroP $\delta^{15}N$ was calculated as:

$$\begin{split} \delta^{15} N_{micro} &= \\ & (\delta^{15} N_{200} - ((\delta^{15} N_{nano} \times F_{nano200}) + (\delta^{15} N_{pico} \times F_{pico200}))) / F_{micro200} \end{split}$$

where $\delta^{15}N_{200}$ is $\delta^{15}N$ measured on the < 200- μ m filters, $F_{nano200}$ is the fraction of nanoP Chl on the < 200- μ m filters, $F_{pico200}$ is the fraction of picoP Chl on the < 200- μ m filters, and $F_{micro200}$ is the fraction of microP Chl on the < 200- μ m filters. For two timepoints where microP Chl was zero, microP $\delta^{15}N$ could not be determined.

To analyze plankton taxonomic community composition, WSW samples from each sampling timepoint were preserved (5% Lugol's iodine) for identification and enumeration via microscopy. The bottles were stored at room temperature in the dark until analysis. Volumes of 15–20 mL from each preserved sample were settled for approximately 24 h in settling chambers (Utermöhl 1958) and counted in 20 fields of view using the × 10 objective (× 100 total magnification) on an inverted microscope (Nikon Diaphot-TMD). MicroP and microzooplankton cells were identified to genus when possible or, otherwise, to taxonomically, morphologically, and/or size-consistent groups.

Statistical Analyses

Percent use of the ¹⁵NO₃⁻ tracer or recycled ¹⁵NH₄⁺ by each phytoplankton size class was estimated using simple mixing models. Separate calculations were performed for TSA and creek flooding periods. Percent ¹⁵NO₃ tracer use was calculated using an approximate $\delta^{15}N$ of newly fixed marine N (0.1 %o; Sigman et al. 2009) as the "oceanic" end-member, representing N obtained outside the study creek, and mean surface water $\delta^{15}NO_3^-$ at the sampling site during TSA or creek flooding as the "creek" end-member, representing N originating within the creek. Percent creek-derived ¹⁵NH₄+ use was calculated using mean $\delta^{15}NH_4^+$ measured a few meters seaward of the ¹⁵N addition site during flood tides at salinities > 30 psu (4.87 %o; n = 6) as the "oceanic" endmember, and mean surface water $\delta^{15}NH_4^+$ at the sampling site during TSA or creek flooding as the "creek" end-member. The mean estimate for "oceanic" δ¹⁵NH₄ used may have been



influenced by the tracer addition; however, it was the best estimate that could be calculated from the available data. These simple models assumed steady-state conditions and only 2 possible sources for each N form: external (i.e., imported with flooding tide) or internal (i.e., the added tracer or creekgenerated $\mathrm{NH_4}^+$). It is important to note that due to the short residence time of phytoplankton in the study creek, which emptied completely with each ebb tide, phytoplankton $\delta^{15}\mathrm{N}$ and nutrient uptake calculations could be complicated by differences in time spent in waters with lower proportions of tracer downstream of the study creek, versus in the creek with direct tracer exposure.

Percent use of the external and creek-derived ¹⁵NO₃⁻ or ¹⁵NH₄⁺ was estimated using a system of equations:

$$\begin{split} \delta^{15} N_{phyto} &= \left(\delta^{15} N_{extemal} \times P_{extemal}\right) \\ &+ \left(\delta^{15} N_{intemal} \times P_{intemal}\right) \end{split}$$

 $P_{\text{external}} + P_{\text{internal}} = 1$

where $\delta^{15}N_{phyto}$ is the $\delta^{15}N$ value of each phytoplankton size class, $\delta^{15}N_{external}$ is the estimate of downstream "oceanic" $\delta^{15}NO_3^-$ (0.1 ‰) or $\delta^{15}NH_4^+$ (4.87 ‰), $\delta^{15}N_{internal}$ is the mean $\delta^{15}NO_3^-$ or $\delta^{15}NH_4^+$ value from the TSA or creek flooding period, $P_{external}$ is the percent use of external ^{15}N , and $P_{internal}$ is the percent use of creek-derived $^{15}NO_3^-$ or $^{15}NH_4^+$. While these models do not include other potential N sources, such as DON, they serve as a simple way to estimate the degree to which phytoplankton were using N in the creek versus N from downstream of the study site. Values of percent $^{15}NH_4^+$ use may be underestimated because the model does not account for ammonification to uptake of $^{15}NH_4^+$, which was not measured.

Model II ordinary least squares regression was performed using the R package "lmodel2" (Legendre 2018; R Core Team 2020) to compare size-specific plankton $\delta^{15} N$ with water column NH_4^+ concentration and with size-specific Chl over tidal cycles. High tide measurements were defined as those measured at water heights within 0.2 m of the highest recorded water height for each diurnal tidal cycle. All error terms reported with means are standard error.

Results

Environmental Conditions

Over the duration of the study, West Creek emptied almost completely at each low tide, and one rainstorm occurred on day 200. The proximity of the sampling site to the landward end of the creek reach meant that the upstream end of the study site was relatively closed off, and the majority of water input was from downstream. Surface water concentrations of NO₃⁻

were generally higher during creek flooding (mean 12.51 ± 1.57 μ M) than TSA flooding periods (mean 8.19 \pm 1.08 μ M; Table 1). Similarly, concentrations of NH₄⁺ were generally higher during creek flooding (mean $11.15 \pm 1.69 \mu M$) than TSA flooding periods (mean $9.36 \pm 1.26 \mu M$; Table 1). Concentrations of NO₃⁻ and NH₄⁺ were similar to each other and changed relatively in-phase with each other during the first half of the study (days 192-197), after which they showed an inverse relationship to each other (days 198-202; Fig. 2a). Concentrations of PO₄³⁻ were generally much lower than either form of N, ranging from 0.9-2.8 µM over the duration of tracer addition (Fig. 2a, diamonds). The average ratio of DIN to DIP was below the Redfield ratio of 16:1 (Redfield 1958) throughout the experiment (Table 1). Overall, concentrations of N were similar at the start and end of the experiment, suggesting that tracer addition did not lead to general N enrichment in the system during the study period.

Throughout the experiment, DO generally increased during flood tides as water levels rose (Fig. 2b). During creek flooding tides, DO was more variable, with lower minima during ebb tide followed by higher maxima at early flood tide (Fig. 2b, gray area). Salinity varied between 23 and 31 psu during the experiment, though five brief decreases to 3–17 were observed at low tides, primarily during the period of creek flooding (Fig. 2c). It is likely that these short periods of low salinity were due to small freshwater inputs and/or reduced conductivity sensor accuracy when creek water volume was negligible. Despite these decreases, mean salinity measured during phytoplankton sampling timepoints (28.32 \pm 0.54 and 29.05 \pm 0.34 during TSA and creek flooding periods, respectively) was within one unit of average salinity in

Table 1 Mean, standard error (S.E.), and sample number (*n*) for environmental variables during TSA flooding (mid tide) and creek flooding (neap tide) periods. Phosphate and DIN:DIP *n* values are lower during TSA flooding because phosphate was not sampled on day 202. Total suspended solids and current speed were only measured on days 193, 194, 196, 198, and 202. Mean current speed was calculated from values measured by ADCP within 30 min preceding each sampling timepoint during flood and ebb tides (i.e., excluding high tide samples)

	TSA flooding			Creek flooding		
	Mean	S.E.	n	Mean	S.E.	n
Nitrate (µM)	8.19	1.08	10	12.51	1.57	9
Ammonium (µM)	9.36	1.26	10	11.15	1.69	10
Phosphate (µM)	1.34	0.11	6	2.10	0.12	10
DIN:DIP	13.72	1.84	6	11.21	0.79	9
Temperature (°C)	23.72	0.67	10	25.28	0.25	10
Salinity (psu)	28.32	0.54	10	29.05	0.34	10
Dissolved oxygen (mg L ⁻¹)	5.57	0.30	10	4.68	0.47	10
Total suspended solids (mg L^{-1})	46.73	6.80	8	38.26	5.31	5
Current speed (m s ⁻¹)	0.053	0.003	64	0.039	0.002	46



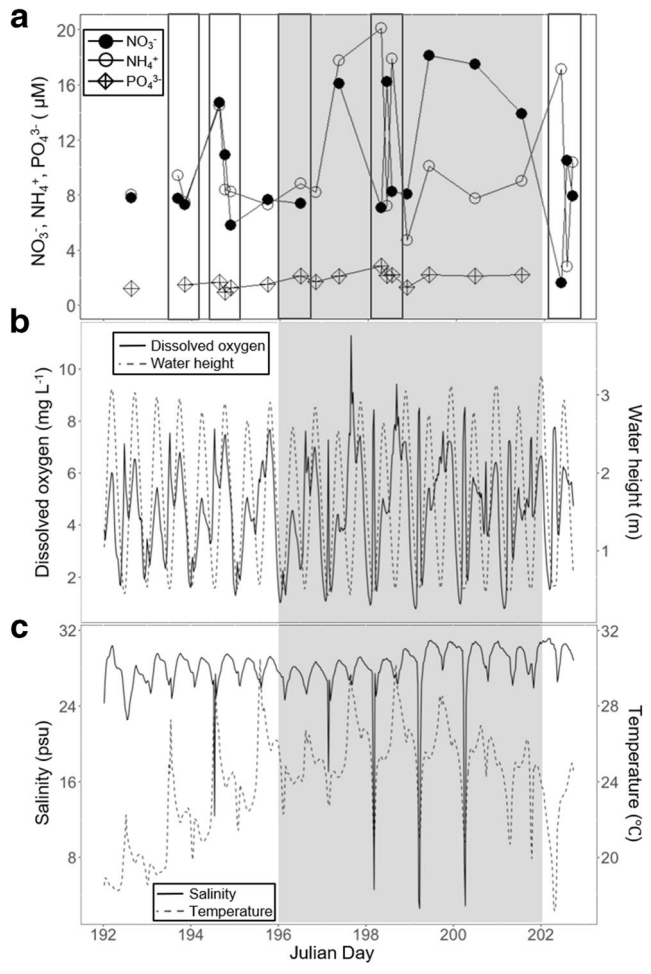
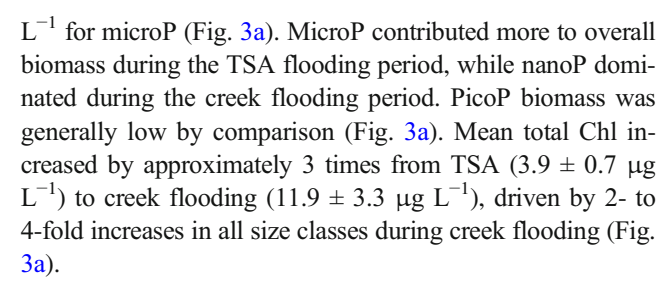


Fig. 2 Surface nutrient concentrations and environmental conditions over the duration of the experiment. A: concentration of NO_3^- (filled circles), NH_4^+ (open circles), and PO_4^{3-} (crossed diamonds). B: dissolved oxygen (solid line) and water height (dashed line). C: salinity (solid line) and temperature (dashed line). Gray shading in all panels represents days during neap tide when only the creek was flooded at high tide. Rectangles in panel A represent periods when data were collected throughout the diumal tidal cycle

the outer estuary of Plum Island Sound (29.1 \pm 0.9; Deegan et al. 2007). Mean water temperature measured during phytoplankton sampling timepoints was approximately 1.5 °C higher during creek (25.28 \pm 0.25 °C) than TSA flooding periods (23.72 \pm 0.67 °C; Table 1). In terms of physical mixing, mean current speed measured within 30 min preceding phytoplankton sampling timepoints during flood and ebb tides (excluding high tides) was lower during creek (0.039 \pm 0.002 m s⁻¹) than TSA flooding tides (0.053 \pm 0.003 m s⁻¹; Table 1). TSS was also lower during creek (38.26 \pm 5.31 mg L⁻¹) than TSA flooding tides (46.73 \pm 6.80 mg L⁻¹; Table 1).

Phytoplankton Biomass and Community Composition

Throughout the study, Chl ranged between 0.3 and 2.7 μ g L⁻¹ for picoP; 0.1 and 28.9 μ g L⁻¹ for nanoP; and 0.2 and 11.5 μ g



Within the microplankton, a shift in community composition occurred from TSA to creek flooding, with dinoflagellates and dinoflagellate cysts increasing in relative abundance in the latter (Fig. 4). This shift is attributable, in part, to dinoflagellates in the genus Alexandrium, which were generally dominant in the microP assemblage and nearly doubled in mean relative abundance from TSA (25.2%) to creek flooding (47.4%; Table 2). Alexandrium spp. also showed higher maximum relative abundances during ebb tides throughout the experiment (Table 2). Pennate diatoms (dominated by Navicula spp.) also contributed to the assemblage, with mean relative abundance decreasing from TSA (31.6%) to creek flooding (10.3%; Table 2, Fig. 4). Microzooplankton were also enumerated, the majority of which (92%) belonged to the genus of aloricate ciliates Strombidium. Relative abundance of these ciliates decreased by approximately half (20.5-11.5%) over the course of the study (Table 2, Fig. 4) but showed little change over diurnal tidal cycles within each flooding regime (Table 2). The dinoflagellate cysts that were observed were primarily ecdysal (or pellicle) cysts. These cysts comprised 13.6%, on average, of the microplankton communities during creek flooding but contributed < 1% to the total community during TSA flooding (Table 2).

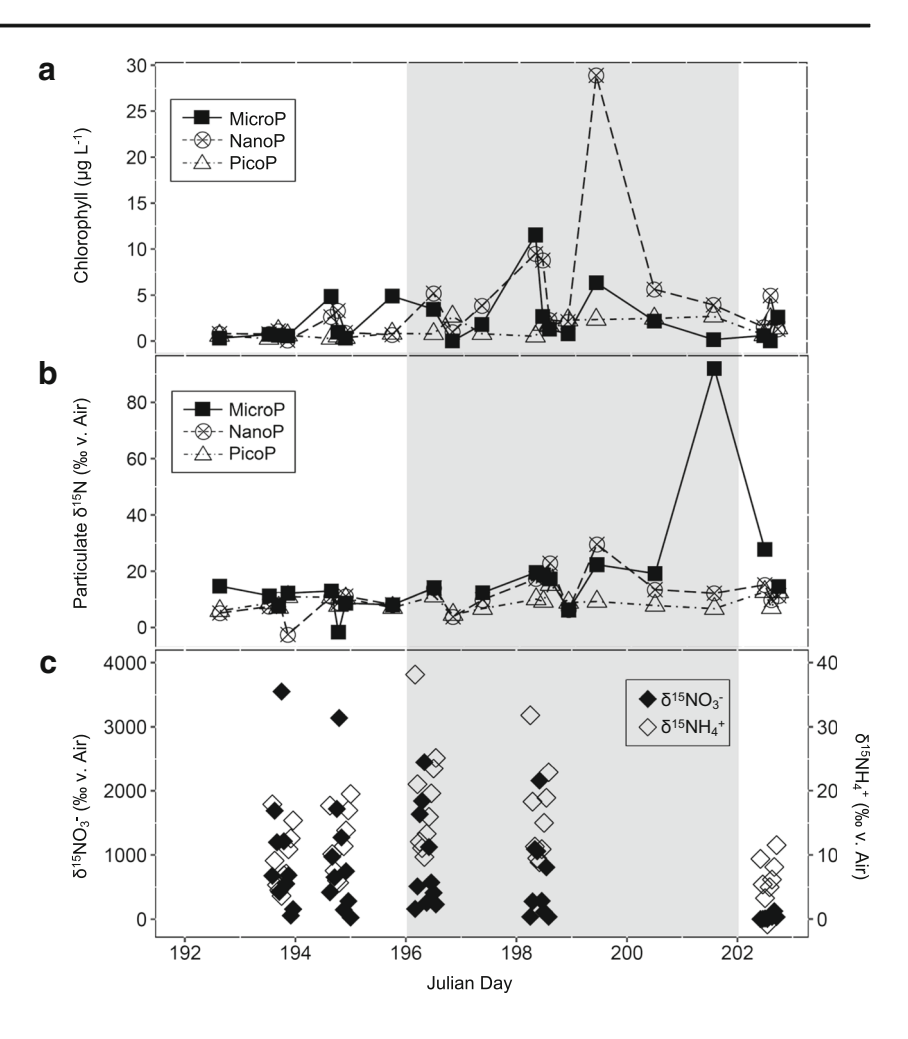
N Use by Phytoplankton Size Classes

In addition to changes in biomass, size-based phytoplankton groups showed distinct particulate $\delta^{15}N$ values over the experiment (Fig. 3b). PicoP showed the smallest range in δ^{15} N (5.9-15.2 %), while nanoP (- 2.5-29.5 %) and microP (-1.7-27.8 %, excluding high outlier on day 201) had larger ranges and considerably higher maxima (Fig. 3b). The nanoP δ^{15} N maximum on day 199 (29.5 %; Fig. 3b) coincided with maximal nanoP biomass on that day (28.9 μ g L⁻¹; Fig. 3a). Mean microP δ^{15} N increased from TSA (11.6 \pm 2.3 %) to creek flooding (16.2 \pm 1.8 %; excluding day 201). Mean nanoP $\delta^{15}N$ showed a greater increase than microP from TSA $(8.6 \pm 1.4 \%)$ to creek flooding $(14.7 \pm 2.4 \%)$, while mean picoP δ^{15} N changed little from TSA (9.1 \pm 0.7 %) to creek flooding (8.9 \pm 0.9 %). Unlike water column δ^{15} N, particulate δ^{15} N did not decrease substantially in the 1 day following the end of ¹⁵N addition (Fig. 3b, day 202).

Mean water column $\delta^{15} NO_3^-$ was 1021 ‰ during TSA flooding (excluding day 202) and 792 ‰ during creek flooding, while mean $\delta^{15} NH_4^+$ was 10.6 ‰ during TSA



Fig. 3 Chlorophyll (A) and $\delta^{15}N$ (B) over the duration of the experiment for microphytoplankton (microP: filled squares/solid line), nanophytoplankton (nanoP; crossed circles/dashed line), and picophytoplankton (picoP; open triangles/dot-dash line). C: surface water $\delta^{15}NO_3^-$ (filled diamonds) and $\delta^{15}NH_4^+$ (open diamonds), as measured over five diurnal tidal cycles. Gray shading represents days during neap tide when only the creek was flooded at high tide



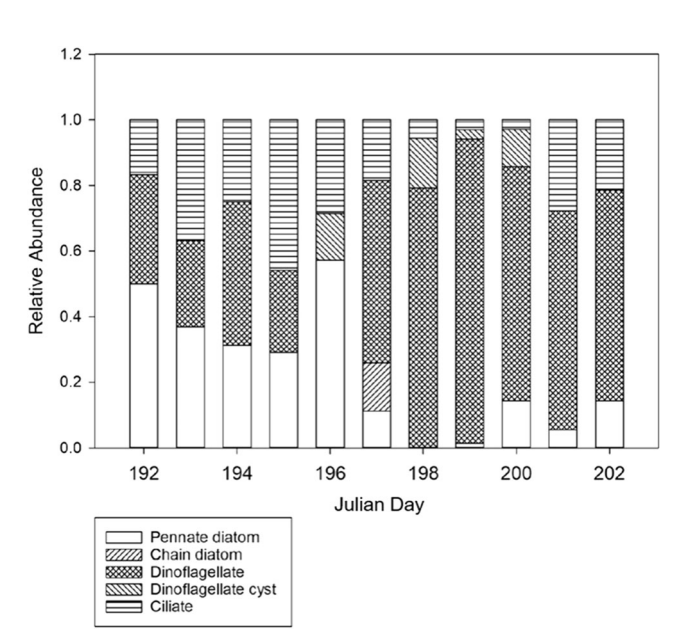


Fig. 4 Relative abundances of major taxonomic groups in the microplankton at or near high tide for each day of the experiment. Bar patterns represent taxonomic groups, including pennate diatoms, chainforming diatoms, dinoflagellates, dinoflagellate cysts, and ciliates

flooding (excluding day 202) and 17.7 % during creek flooding (Table 3). Water column $\delta^{15}NO_3$ reached maximum values of 3550 % and 2448 % during TSA and creek flooding, respectively, and typically centered around high tide (Fig. 3c) due to the continuous addition of tracer during flood tide. After cessation of tracer addition at high tide, $\delta^{15}NO_3^{-1}$ decreased steadily due to a combination of biotic uptake, tidal export, and other removal processes (e.g., Tobias et al. 2003a). Water column $\delta^{15}NH_4^+$ reached maximum values of 17.9 % and 38.1 % during TSA and creek flooding, respectively (Fig. 3c), and typically centered around low tide (i.e., during early flood and late ebb stages of the diurnal cycle). In contrast with $\delta^{15}NO_3^-$, $\delta^{15}NH_4^+$ was minimal around high tide (Fig. 3c). On day 202 after the end of 15N addition, water column δ¹⁵NO₃ maximum values decreased approximately an order of magnitude, while maximum water column $\delta^{15}NH_4^+$ only decreased by half (Fig. 3c).

Percent use of the $^{15}NO_3^-$ tracer by each size class was estimated using simple mixing models, with an approximate $\delta^{15}N$ value of newly fixed oceanic ^{15}N (0.1 ‰) determined from literature (Sigman et al. 2009) representing the "external" end-member. Mean water column $\delta^{15}NO_3^-$ values from



Table 2 Mean relative abundance (%) of dominant microphytoplankton and microzooplankton taxa over the entire experiment, and range of relative abundances (%) for those taxa at flood, high, and ebb tide during TSA flooding (mid tide) and creek flooding (neap tide) periods. The taxa

given here represent those that contributed > 5% to overall community composition. Number of samples for each period (n) is given in parentheses in column headings

Taxon	TSA floodi	TSA flooding			Creek flooding			
	Mean (9)	Flood (5)	High (2)	Ebb (2)	Mean (10)	Flood (4)	High (4)	Ebb (2)
Alexandrium spp. (dinoflagellate)	25.2	16.7–26.3	28.6–35.9	0-70.3	47.7	51.4–79.7	0-62.5	51.8–92.0
Scrippsiella sp. (dinoflagellate)	7.1	0-16.7	5.4-35.7	0	10.8	0-20.0	0-37.0	0-12.5
Dinoflagellate ecdysal cyst	0.20	0-1.8	0	0	13.6	0-11.5	0-66.7	0-16.1
Navicula spp. (diatom)	12.0	0-36.4	5.4-7.1	0	3.7	0-5.7	0-12.5	3.6-4.0
Unid. pennate diatom	19.6	10.5-50.0	7.1 - 12.0	11.1-27.3	6.6	0-5.7	0-37.5	0-1.8
Strombidium spp. (ciliate)	20.5	1.8-45.8	21.4–23.9	11.1–36.4	11.5	2.9-27.8	5.6-25.0	0-5.4

TSA flooding or creek flooding were used to represent the creek-derived end-members in the mixing models. Model results suggest that the phytoplankton groups used specific forms of N, from different origins, and with only some changes at different stages of the tidal cycle. During TSA flooding, all three size classes obtained between 0.7% and 0.9% (Table 3) of their ¹⁵N, on average, from the ¹⁵NO₃⁻ tracer. All three groups obtained slightly larger proportions (1.1–2.0%; Table 3) of their ¹⁵N from the tracer during creek flooding, but overall tracer uptake was low throughout the experiment.

The same mixing model method was used to estimate size-specific percent uptake of recycled $^{15}{\rm NH_4}^+$, using mean $\delta^{15}{\rm NH_4}^+$ measured just seaward of the tracer addition site at salinities > 30 psu (4.87 ‰) as the external end-member and mean water column $\delta^{15}{\rm NH_4}^+$ during TSA or creek flooding as

Table 3 Mixing model estimates of mean percent contribution of ^{15}N tracer-labeled NO_3^- and NH_4^+ to the $\delta^{15}N$ of microP, nanoP, and picoP during TSA and creek flooding periods. Calculations for $^{15}NO_3^-$ contribution were done using the approximate value of newly fixed marine N (Sigman et al. 2009) as the "oceanic" end-member, and mean surface water $\delta^{15}NO_3^-$ at the sampling site as the "creek" end-member. Calculations for $^{15}NH_4^+$ contribution were done using mean $\delta^{15}NH_4^+$ measured just seaward of the ^{15}N addition site at salinities > 30 psu as the "oceanic" end-member, and mean surface water $\delta^{15}NH_4^+$ at the sampling site as the "creek" end-member. See "Methods" for more details. Note: Creek flooding microP calculations exclude day 201 sample

	¹⁵ NO ₃ ⁻		15NH	4
	TSA	Creek	TSA	Creek
Estimated "oceanic" δ ¹⁵ N (‰)	0.1	0.1	4.87	4.87
Mean "creek" $\delta^{15}N$ (‰) at sampling site	1021	792	10.6	17.7
MicroP use (%)	0.89	2.03	76.0	88.2
NanoP use (%)	0.71	1.85	43.0	76.9
PicoP use (%)	0.83	1.11	63.8	31.6

the creek-derived end-member. During TSA flooding, picoP obtained 63.8% of their 15 N, on average, from creek-derived 15 NH₄⁺ (Table 3), and picoP δ^{15} N showed a significant positive linear relationship with NH₄⁺ concentration ($n = 10, R^2 = 0.42, 2$ -tailed p = 0.042; Fig. 5a, dashed line). During creek flooding, picoP use of 15 NH₄⁺ decreased by approximately half (Table 3), and the linear relationship between NH₄⁺ and picoP δ^{15} N was not significant (2-tailed p > 0.05; Fig. 5b). In

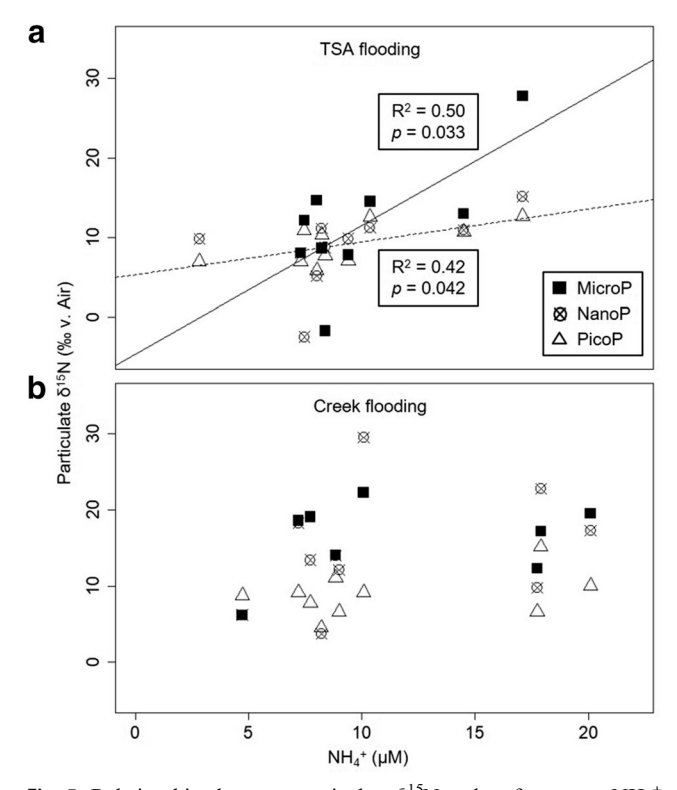


Fig. 5 Relationships between particulate δ^{15} N and surface water NH₄⁺ concentration for microphytoplankton (microP; filled squares), nanophytoplankton (nanoP; crossed circles), and picophytoplankton (picoP; open triangles) during TSA flooding (A) and creek flooding (B). Trendlines show significant linear regressions (p < 0.05) for microP (solid line) and picoP (dashed line)



contrast, nanoP obtained a higher proportion of their ¹⁵N from recycled ¹⁵NH₄⁺ during creek (76.9%) than TSA flooding (43.0%; Table 3), though linear relationships between NH₄⁺ and nanoP δ^{15} N were not significant during either time period (2-tailed p > 0.05; Fig. 5). MicroP consistently obtained higher proportions of ¹⁵N from creek-derived ¹⁵NH₄⁺ than the smaller size classes did, and these contributions increased slightly from TSA (76.0%) to creek flooding (88.2%; Table 3). MicroP δ^{15} N showed a positive linear relationship with NH₄⁺ during only TSA flooding (n = 9, $R^2 = 0.50$, 2-tailed p = 0.033; Fig. 5a, solid line). This result appeared to be driven by a single high NH₄⁺, high microP δ^{15} N point in the dataset, however, and the relationship was no longer significant when that datapoint was removed ($R^2 = 0.084$, 2-tailed p = 0.485).

To determine the degree to which different phytoplankton groups were using 15 N and increasing biomass within the tidal creek, size-specific δ^{15} N and Chl were compared using Model II linear regression. Among samples collected at or near high tide, nanoP δ^{15} N and Chl were significantly and positively correlated during creek flooding (n = 7, $R^2 = 0.89$, 2-tailed p = 0.001; Fig. 6b), but not during TSA flooding (2-tailed p > 0.001)

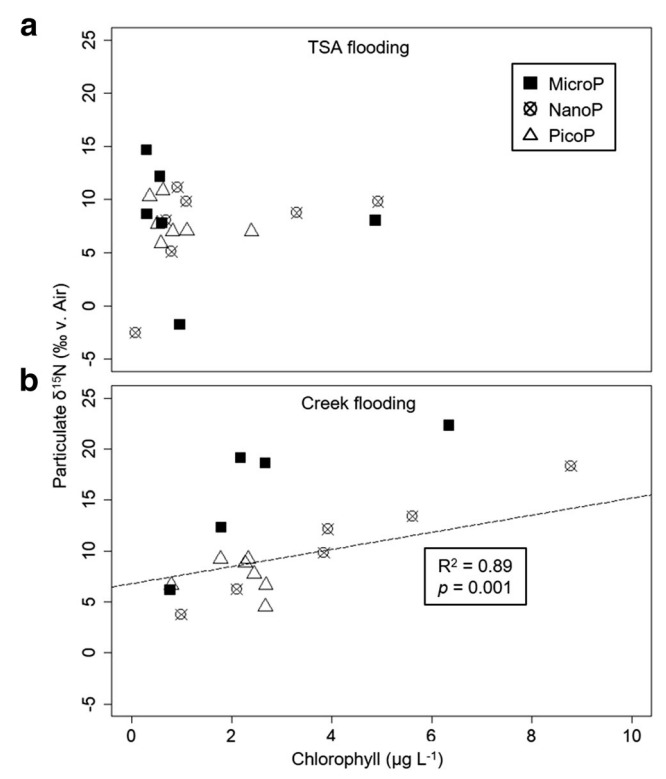


Fig. 6 Relationships between particulate δ^{15} N and chlorophyll (Chl) for microphytoplankton (microP; filled squares), nanophytoplankton (nanoP; crossed circles), and picophytoplankton (picoP; open triangles) for samples collected at or near high tide during TSA flooding (A) and creek flooding (B). Trendline shows significant linear regression (p < 0.05) between nanoP δ^{15} N and Chl. Note: One nanoP datapoint from creek flooding (B) is not shown due to high Chl value that is off-scale, but was still included in the regression analysis

0.05; Fig. 6a). While two high Chl, high $\delta^{15}N$ datapoints influenced this nanoP relationship, the results were still significant even with those datapoints excluded. Chl and $\delta^{15}N$ were not significantly correlated for microP or picoP during either the TSA (Fig. 6a) or creek (Fig. 6b) flooding periods.

During the diurnal tidal cycles that were sampled (5 cycles in total), overall Chl decreased from flood to ebb tide within each cycle (Fig. 7, x-axis). NanoP Chl and δ^{15} N were significantly and positively correlated during both flood (n = 8, $R^2 = 0.87$, 2-tailed p = 0.0007; Fig. 7a) and high tide (n = 7, $R^2 = 0.93$, 2-tailed p = 0.0005; Fig. 7b) stages of the diurnal tidal cycle. PicoP Chl and δ^{15} N were also significantly and positively correlated (n = 5, $R^2 = 0.88$, 2-tailed p = 0.018) but during ebb tide only (Fig. 7c). There were no significant linear relationships between Chl and δ^{15} N for microP during any of the diurnal tidal stages. Bivariate Model II linear regressions also revealed significant positive relationships between picoP

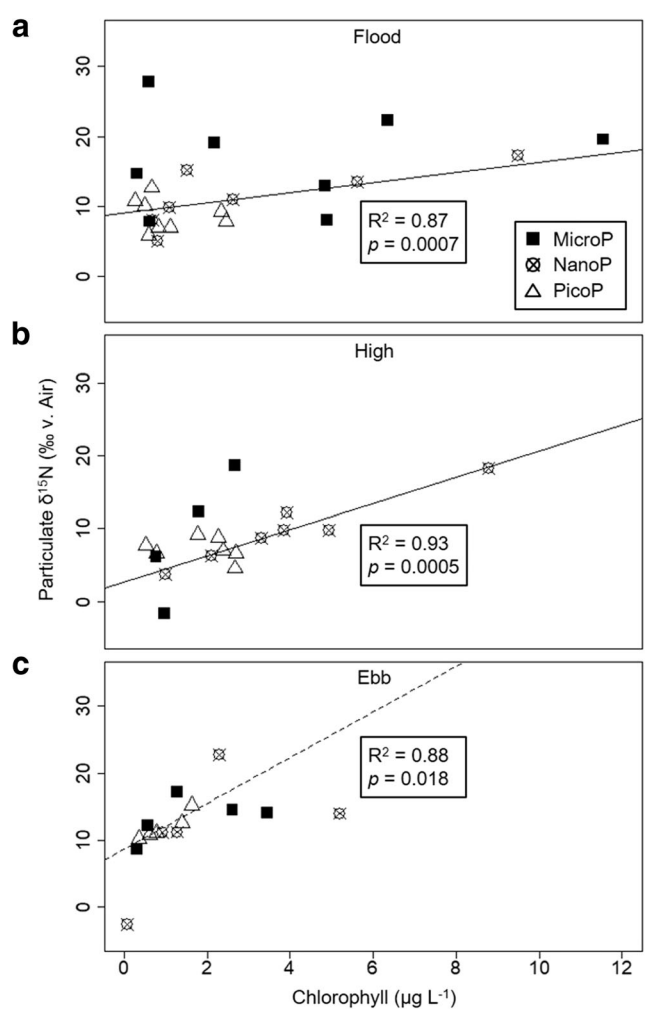


Fig. 7 Relationships between particulate δ^{15} N and chlorophyll for microphytoplankton (microP; filled squares), nanophytoplankton (nanoP; crossed circles), and picophytoplankton (picoP; open triangles) during flood (A), high (B), and ebb (C) tides. Trendlines show significant linear regressions (p < 0.05) for nanoP (solid lines) and picoP (dashed line)



 δ^{15} N and surface NH₄⁺ during flood (n = 8, $R^2 = 0.66$, 2-tailed p = 0.014) and ebb tides (n = 5, $R^2 = 0.94$, 2-tailed p = 0.007), but not at high tides (n = 7, 2-tailed p > 0.05), over the duration of the experiment (Fig. 8). Relationships between NH₄⁺ and particulate δ^{15} N were not observed for nanoP or microP during flood, high, or ebb tides (not shown).

Discussion

Environmental Drivers of Nutrient Dynamics

The middle estuary of PIE is typically characterized by NH_4^+ concentrations of 5–20 μ M, NO_3^- concentrations of 1–10 μ M, and low pelagic Chl (< 5 μ g L^{-1}) during the summer months (Deegan and Garritt 1997). Nutrient and Chl concentrations during the current study reflect these general trends, although NO_3^- and Chl showed higher maximum peaks of 18.1 μ M and 37.6 μ g L^{-1} , respectively. This site is generally N-limited (Deegan et al. 2007), and mean N:P ratio (12.2) during the current study supports this condition, suggesting that changes in phytoplankton ^{15}N uptake were not influenced by P-limitation. Given the generally high concentrations of nutrients overall, other controls (e.g., micronutrients, light, grazing) not quantified in the current study likely had limiting effects on phytoplankton growth in this system.

Surface DIN concentrations were also tidally mediated and were generally lower when the TSA flooded than when only the creek flooded (i.e., periods of neap tide; Fig. 2a). These results fit with previous studies documenting the role of the salt marsh platform as a nutrient sink when it is flooded by high tides (Childers 1994; Vörösmarty and Loder III 1994), though it is worth noting that full spring tide was not experienced during this study. While increased water volumes

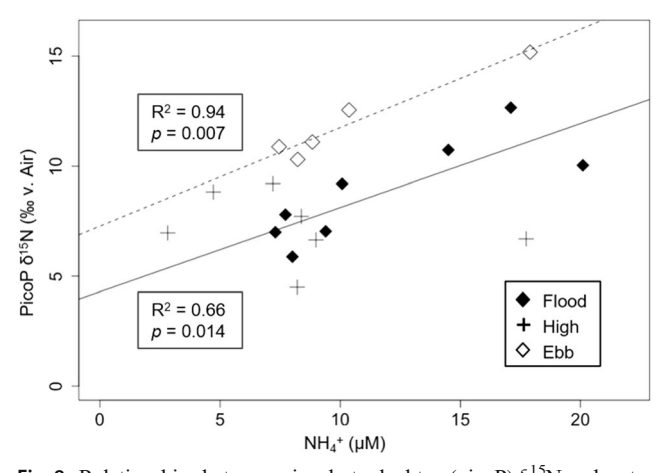


Fig. 8 Relationships between picophytoplankton (picoP) δ^{15} N and water column NH₄⁺ concentration during flood (filled diamonds), high (plus symbols), and ebb (open diamonds) tides. Trendlines show significant linear regressions (p < 0.05) for flood (solid line) and ebb (dashed line) tides

during TSA flooding may have diluted nutrient and plankton concentrations compared to creek flooding (Wetz et al. 2006), evidence suggests spring-neap changes in estuarine biogeochemical processing have a greater effect on nutrient dynamics in this system than dilution alone (Vörösmarty and Loder III 1994). Other PIE studies have reported high rates of NH₄⁺ flux from sediments (3-10 mmol m⁻² day⁻¹; Tobias et al. 2003b; Weston et al. 2010), especially during summer months, demonstrating rapid processing of NH₄⁺ by marsh biota in this system. In the current study, the rise in water column $\delta^{15}NH_4^+$ at low water level during creek flooding also indicates that aside from possible decreased dilution, more ¹⁵NO₃ was being recycled to ¹⁵NH₄ during neap tide, likely due to increased microbial remineralization (Tobias et al. 2003b; Spivak and Ossolinski 2016) and/or dissimilatory NO₃ reduction to NH₄ (Giblin et al. 2013).

Phytoplankton Use of Different N Sources

Based on the results of this study, phytoplankton took up very little of the experimentally-added ¹⁵NO₃⁻ tracer directly, despite the tracer comprising 25–35% of ¹⁵NO₃⁻ in the creek (but < 1% of total NO₃⁻) over the course of the experiment. All three size-based groups of phytoplankton obtained approximately 1–2% of ¹⁵NO₃ from the added tracer, as estimated by simple mixing models (Table 3). These results indicate minimal use of "new" N (i.e., NO₃⁻) from within the creek system by any of the phytoplankton size classes, in contrast to previous findings of rapid, direct ¹⁵NO₃⁻ uptake by phytoplankton in other estuarine isotope tracer experiments (Holmes et al. 2000; Duernberger et al. 2011). These differences could have multiple explanations. For one, both Holmes et al. (2000) and Duernberger et al. (2011) found the highest phytoplankton isotope enrichment in the upper oligohaline zones of their study systems (Parker River, Plum Island, Massachusetts, and Hewlett's Creek, North Carolina, respectively), while the current study focused on the euryhaline middle estuary. These previous studies were also conducted in locations and during time periods with higher phytoplankton biomass and production (Chl 20–100 μ g L⁻¹; Holmes et al. 2000) than the current study (Chl 1–38 μ g L⁻¹;). Duernberger et al. (2011) did not report Chl values but stated that they sampled during the summertime period of "high production." Our results more closely reflect those of Tobias et al. (2003a), which were obtained from a ¹⁵NO₃⁻ tracer experiment conducted in the same middle estuary region of the PIE Rowley River system, with low Chl biomass (2–8 μ g L⁻¹) generally similar to our observations and to interannual Chl variability in the Gulf of Maine (Thomas et al. 2003).

Other possible explanations for our observations of low ¹⁵NO₃⁻ tracer uptake by phytoplankton include high phytoplankton turnover due to growth, grazing loss, and/or short time periods spent in the creek. While Holmes et al. (2000) showed



that phytoplankton became substantially enriched in ¹⁵N (61 %c) within 54 h after the start of ¹⁵NO₃⁻ tracer addition, even with the effects of phytoplankton growth turnover (estimated 1–2 days), water residence time averaged 12 days during that study's tracer addition period. In contrast, summertime water residence time in the middle estuary of the Rowley River system where the current study was conducted is 1.2–1.4 days (Tobias et al. 2003a). Therefore, short residence time in the creek coupled with similar growth rates could contribute to the minimal ¹⁵NO₃⁻ tracer uptake by the phytoplankton community in this system. These results also demonstrate that even within the single estuarine region of PIE, the distinct hydrologic conditions between different river systems and salinity zones may contribute to large differences in the community dynamics and N processing roles of phytoplankton.

There was significantly more evidence for phytoplankton use of recycled forms of N, specifically NH₄⁺, across phytoplankton size groups and over the study period (Table 3). These results are consistent with known preferential uptake of reduced N by many phytoplankton groups (Glibert et al. 2016) and possible inhibitory effects of NH₄⁺ on NO₃⁻ uptake that are well described in the phytoplankton literature (as reviewed in Dortch 1990). The concentrations of NH₄⁺ (6-24 μ M) and NO₃⁻ (5–15 μ M) observed during the current study fit within the range of values that previous studies have associated with at least partial NO₃⁻ uptake inhibition (NH₄⁺ $> 2-5 \mu M$, $NO_3^- < 10 \mu M$; Carpenter and Dunham 1985; Xu et al. 2012). This inhibitory phenomenon could explain, at least in part, the low NO₃ uptake and high reliance on recycled N by phytoplankton in the current study and previous observations of low phytoplankton NO₃⁻ processing in the Rowley River system (Tobias et al. 2003a). In contrast, the low NH_4^+ concentrations (generally < 2 μ M) relative to NO_3^- (4–16 μM) observed by Holmes et al. (2000), combined with high Chl biomass and diatom abundance, indicate less potential for NH₄⁺ inhibition and may have driven high isotope tracer uptake in that study.

Tidally Mediated N Use by Size-Specific Phytoplankton Groups

Despite the expectation that microP preference for NO_3^- (e.g., Probyn and Painting 1985; Glibert et al. 2016) would result in enhanced $^{15}NO_3^-$ uptake in the experimental creek (and thus higher $\delta^{15}N$), and despite frequent substantial peaks in microP biomass during the experiment (Fig. 3a), microP did not appear to use NO_3^- from within the creek during either TSA or creek flooding. Rather, microP $\delta^{15}N$ values indicated a predominant reliance on NH_4^+ , and potentially other forms of recycled N, in the creek throughout the experiment. These results reflect overall phytoplankton preference for NH_4^+ over NO_3^- under nutrient-replete conditions (Glibert et al. 2016 and references therein) and the effects of NO_3^- uptake

inhibition by NH₄⁺ (L'Helguen et al. 2008). The comparably high use of NH₄⁺ between microP and the smaller phytoplankton size groups also fits with other studies that have found either no relationship between NH₄⁺ uptake and cell size (Stolte et al. 1994) or minimal difference in microP preference for NH₄⁺ versus NO₃⁻ (Wafar et al. 2004). While we did not measure DON in the current study, DON and other forms of remineralized N generated in the creek could have also contributed to microP N uptake, particularly by dinoflagellates in this size group (Bronk et al. 2007) and during creek flooding when microP δ^{15} N was not correlated with NH₄⁺ concentration (Fig. 5b). It is important to note that contamination of the < 200-µm filters with detritus, sediment, or heterotrophic/mixotrophic cells could have affected microP δ^{15} N measurements. However, the substantial peaks in microP Chl provide reasonable evidence to attribute the bulk of δ^{15} N signal to microP.

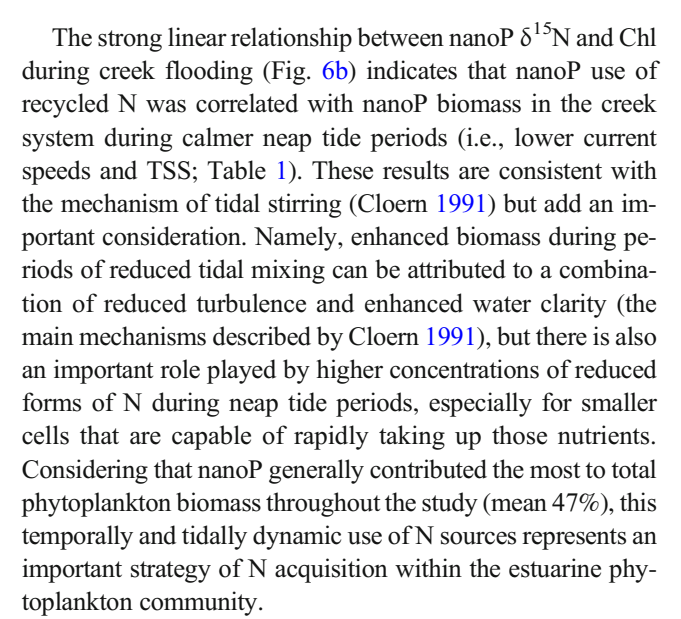
Despite the consistently low use of NO₃⁻ and high use of recycled N from within the creek by microP throughout the experiment, we observed substantial changes in community composition over the mid-neap tidal cycle. The observation of relatively high diatom abundance during TSA flooding (Fig. 4), coupled with substantial use of creek-derived ¹⁵NH₄+ (76%; Table 3) by microP during TSA flooding, indicates that diatoms in this system primarily used recycled N. While diatoms are generally thought to prefer NO₃ (Glibert 2016), our results reflect other findings in temperate estuaries of enhanced diatom growth in response to increased concentrations of regenerated N forms (e.g., Koch and Gobler 2009; Tada et al. 2009). The dominance of *Navicula* spp. among diatoms identified in the current study (Table 2) also reflects previous evidence of some Navicula species growing well at high NH₄⁺ concentrations (Underwood and Provot 2000), and increased abundance of this typically benthic genus during TSA flooding, as compared with creek flooding, provides support for greater mixing and benthic resuspension during TSA flooding. Generally, diatom abundances decreased, and dinoflagellate abundances increased from TSA to creek flooding (Fig. 4), changes that are consistent with previous observations in the Gulf of Maine by Balch (1981) and the more general "tidal stirring" concept (Cloern 1991; Teixeira et al. 2014). Cloern (1991) attributes enhanced biomass and increased abundance of dinoflagellates, both of which we observed (Fig. 3a; Fig. 4), to periods of increased water column stability and clarity during neap tide. Decreased current speeds and TSS during creek flooding (Table 1) in the current study, indicative of these neap tide conditions, may have contributed to the community changes we observed.

In addition to a general microP biomass increase, we observed an approximate doubling of *Alexandrium* spp. abundance from TSA to creek flooding (Table 2), even though microP use of the ¹⁵NO₃⁻ tracer remained low and use of creek-derived ¹⁵NH₄⁺ increased by only 16% during this



transition (Table 3). These results suggest that the growth of these potentially toxic dinoflagellates in estuaries may not depend solely on local DIN availability. DIN storage capacity in multiple *Alexandrium* species (Collos et al. 2004; Fauchot et al. 2005; Maguer et al. 2007), consistent with the low ¹⁵NO₃ use by microP that we observed, points to the need to consider drivers of Alexandrium blooms—including nutrients (e.g., Fauchot et al. 2005; Ralston et al. 2015)—beyond the hyperlocal coastal and estuarine systems in which they are observed (Anderson et al. 2005). It is also possible that the ability of this dinoflagellate genus (and other dinoflagellate and ciliate genera observed) to use organic sources of carbon and nitrogen for growth (i.e., mixotrophy; e.g., Jeong et al. 2010) contributed to changes in biomass and/or microP δ^{15} N. especially during creek flooding when these taxa were numerically dominant. Mixotrophy or heterotrophy in the microplankton could also explain the lack of significant correlation between microP Chl and δ^{15} N over the duration of the experiment. While it was not possible to quantify the extent to which the Alexandrium spp. observed were growing mixotrophically within the scope of the current study, other studies have shown that the use of organic N by mixotrophic plankton can have significant effects on the isotopic signatures (e.g., Terrado et al. 2017) and should be considered in future studies.

Within the phytoplankton community, N use by nanoP and picoP showed larger changes during the experiment compared with microP, demonstrating the importance of phytoplankton < 20 µm in size to variability in water column estuarine N cycling. NanoP $\delta^{15}N$ during TSA and creek flooding periods suggested minimal use of the ¹⁵NO₃⁻ tracer and at least partial reliance on NH₄⁺, and possibly other recycled N sources, within the study creek. The 79% increase in estimated creekderived 15NH₄+ use by nanoP from TSA to creek flooding periods suggests a decrease in the use of downstream N sources with lower $\delta^{15}N$ during the experiment. While observations of nutrient storage in nanoP, specifically, are currently limited in the literature, our mixing model results suggest that nanoP may have relied partly on internally stored N during TSA flooding (low δ^{15} N; Stolte and Riegman 1995; Lomas and Glibert 2003) and increased uptake of creek-derived ¹⁵NH₄⁺ during creek flooding (Table 3). This change in nanoP N use may be partly explained by community turnover and/or rapid depletion of internal N stores as growth rates increased, leading to size-specific N-limitation (Pedersen and Borum 1996). Given the generally higher concentrations of NH₄⁺ during creek (mean 11.2 μM) than TSA flooding (mean 9.4 μM; Table 1), a combination of increased NH₄⁺ availability, inhibition of NO₃ uptake (see discussion above), and cell turnover could explain this change in N use by nanoP. It is worth noting that many different taxa with different growth rates were integrated into each size class, and this diversity likely complicated the relationships between cell turnover and ¹⁵N uptake in all three size classes.



PicoP δ^{15} N varied relatively consistently within the 4–12 %orange (Fig. 3b). These results suggest that picoP primarily used N that had been processed by other organisms in the estuary, such as that excreted by marsh macrophytes (generally 4-8 %) or consumers (generally 8–12 %o) in the study creek (Deegan and Garritt 1997; Nelson et al. 2015). The reliance of picoP on recycled N sources is consistent with observations of picoplankton (inclusive of auto- and heterotrophs) preference for reduced and/or organic N sources (Harrison and Wood 1988; Probyn et al. 1990) and NO₃ uptake inhibition by NH₄+ in picoautotrophs (mainly picoeukaryotes and cyanobacteria; L'Helguen et al. 2008). Based on mixing model results, the contribution of recycled ¹⁵NH₄⁺ to picoP δ¹⁵N decreased by half from TSA to creek flooding periods (Table 3) despite an approximate doubling of picoP biomass during this period. Based on the near doubling of nanoP use of creek-derived ¹⁵NH₄⁺ over this same time period, it is possible that nanoP began to outcompete picoP for NH₄⁺ during creek flooding, causing picoP to obtain more N from alternative sources such as DON or internal stores. The significant linear relationship between NH₄⁺ and picoP δ^{15} N during TSA (Fig. 5a) but not creek flooding (Fig. 5b) provides additional evidence for a shift in picoP N sources during the

PicoP δ^{15} N was also positively correlated with NH₄⁺ during both flood and ebb tides (Fig. 8) and with picoP Chl during ebb tide (Fig. 7c). Together, these results suggest that picoP use of recycled N forms was regulated, at least to some extent, by the diurnal flood-ebb cycle of advection (i.e., into the creek from the mid-estuary) and biogeochemical cycling (i.e., seepage of reduced N from marsh sediment as during ebb tide; Koch and Gobler 2009). Such results are consistent with observations of highest abundances of *Prochlorococcus*, an important picocyanobacteria genus, during high tides in a Brazilian estuary (Affe et al. 2018) and detectable, yet minimal, effects of the diurnal tidal cycle on phytoplankton biomass and diversity



(which included picoplankton groups) predicted by a model-based study of the macrotidal Iroise Sea in the North Atlantic (Cadier et al. 2017).

One possibly confounding factor in our interpretation of size-specific N use is the extent to which combined communities of auto- and heterotrophic groups, as well as detritus or sediment, contributed to the size fractions. For example, GF/F filters can retain substantial amounts of heterotrophic bacteria (Probyn et al. 1990), which may obscure our ability to definitively attribute the bulk of the ¹⁵N signal to autotrophic (versus heterotrophic) members of the picoP (Fouilland et al. 2007) and could explain the lack of correlation between picoP Chl and δ¹⁵N during TSA and creek flooding periods. The Gulf of Maine contains an abundance of heterotrophic bacteria < 0.8 µm in size (Li et al. 2011), and Hopkinson et al. (1998) documented high growth rates of bacterioplankton using benthic derived inorganic N in PIE. We also observed several putative mixotrophic members of the microP community (Alexandrium, Scrippsiella, and Strombidium spp.; Table 2) that likely contributed substantially to the microP biomass and δ^{15} N, especially during creek flooding (Fig. 4). While we could not definitively quantify the extent to which these organisms were using inorganic versus organic sources of carbon in the current study, this flexibility in nutritional mode is an important consideration in the interpretation of the results. Similarly, heterotrophic members of the nanoplankton which were not enumerated in the current study but can exceed 10³ cells ml⁻¹ in temperate estuaries (Capriulo et al. 2002) likely contributed to the nanoP δ^{15} N. Unfortunately, it was not possible to separately quantify the contributions of mixo- and heterotrophic members to the integrated $\delta^{15}N$ in any of these size classes. However, the significant positive correlation between overall phytoplankton $\delta^{15}N$ (inclusive of all three size fractions) and total Chl ($n = 21, R^2 = 0.59, 2$ -tailed $p = 5 \times 10^{-5}$) suggests that much of what was measured was attributable to pigment-containing autotrophs, as opposed to heterotrophs or sediment/detritus. This correlation was also significant for nanoP specifically, suggesting an insubstantial effect of heterotrophic nanoplankton on $\delta^{15}N$ in this size class. Additionally, Chl biomass (indicating autotrophic plankton) increased approximately two- to four-fold for all three size classes from mid to neap tide, indicating active autotrophic assemblages in PIE. The contributions of mixo- and heterotrophic members of the plankton community to N cycling in estuaries—in addition to autotrophs—thus represent an ongoing knowledge gap that merits further investigation. Differences in the ratio of C to cellular biovolume (e.g., Verity et al. 1992; Menden-Deuer and Lessard 2000) and C:Chl (e.g., Hunter and Laws 1981; Sathyendranath et al. 2009) among and within the phytoplankton size groups could also limit the interpretation of sizespecific δ^{15} N and N uptake from different sources in these groups. However, without the ability to specifically probe individual cells or populations for the uptake of different forms of

N (e.g., as recently done by Berthelot et al. (2019) using cell sorting coupled with nanoSIMs for picocyanobacteria populations), resolving N uptake in natural plankton communities requires integration across different rates of growth and cellular C content in these diverse populations.

Conclusions

The current study found that overall ¹⁵NO₃⁻ tracer uptake by phytoplankton within a tidal creek of PIE was low, consistent with some previous ¹⁵N tracer studies in this system (Tobias et al. 2003a; Drake et al. 2009), and that use of regenerated N sources was more prevalent. By resolving the differences in how the phytoplankton community obtained N from distinct sources within or, putatively, outside of the estuary over the study period, we show that these N uptake dynamics are highly variable across the size-based community and between dominant tidal cycle periods (i.e., spring-neap or flood-ebb). The duration of this study only allowed for observation of these trends over a single spring-neap cycle, and additional studies covering multiple spring-neap cycles are needed to determine if the phytoplankton community's lack of NO₃⁻ uptake and reliance on reduced N remain consistent.

The changes we observed in nanoP and picoP N source from mid to neap tide demonstrate that tidally-varying physical and biogeochemical drivers influence N uptake by these size-specific phytoplankton groups. These results show the important contributions of these < 20-µm groups, which are missed in typical net sampling, to N cycling in the estuary. In addition, the consistently high reliance of larger microplankton on recycled N from within the estuary, despite a shift from a diatom- to dinoflagellate-dominance, highlights the ability of different microplankton assemblages in this system to grow using recycled N. Our findings suggest that recycled N forms within the estuary and those from sources outside of the estuary—more so than local NO₃ concentrations—are important drivers of phytoplankton N uptake dynamics over tidal time scales. This has important implications for phytoplankton bloom dynamics, estuarine and coastal food webs, and estuarine ecosystems experiencing inputs of a variety of N forms from anthropogenic sources (Glibert et al. 2016).

Acknowledgements We thank the research assistants who provided field and laboratory support, M. Otter for isotopic analysis, and two anonymous reviewers whose comments greatly improved the quality of the manuscript.

Funding BAS and JWB received funding for this research from the National Oceanic and Atmospheric Administration (NA16NOS0120017) and Louisiana Sea Grant College Program (NA14OAR4170099). Funding for this study, the Plum Island Ecosystems LTER, and the TIDE project was also provided by the National Science Foundation (NSF-OCE 1238212, NSF-DEB 1354494, NSF-OCE 1233678).



References

- Affe, H.M.J., J. Rigonato, J.M.C. Nunes, and M. Menezes. 2018. Metagenomic analysis of cyanobacteria in an oligotrophic tropical estuary, South Atlantic. Frontiers in Microbiology 9: 1393. https:// doi.org/10.3389/finicb.2018.01393.
- Anderson, D.M., B.A. Keafer, W.R. Geyer, R.P. Signell, and T.C. Loder. 2005. Toxic Alexandrium blooms in the western Gulf of Maine: The plume advection hypothesis revisited. *Limnology and Oceanography* 50 (1): 328–345.
- Balch, W.M. 1981. An apparent lunar tidal cycle of phytoplankton blooming and community succession in the Gulf of Maine. Journal of Experimental Marine Biology and Ecology 55 (1): 65– 77
- Berthelot, H., S. Duhamel, S. L'Helguen, J.-F. Maguer, S. Wang, I. Cetinić, and N. Cassar. 2019. NanoSIMS single cell analyses reveal the contrasting nitrogen sources for small phytoplankton. *The ISME Journal* 13 (3): 651–662.
- Blauw, A.N., E. Benincà, R.W.P.M. Laane, N. Greenwood, and J. Huisman. 2012. Dancing with the tides: Fluctuations of coastal phytoplankton orchestrated by different oscillatory modes of the tidal cycle. *PLoS One* 7 (11): e49319. https://doi.org/10.1371/journal.pone.0049319.
- Bronk, D.A., J.H. See, P. Bradley, and L. Killberg. 2007. DON as a source of bioavailable nitrogen for phytoplankton. *Biogeosciences* 4 (3): 283–296.
- Cadier, M., T. Gorgues, S. L'Helguen, M. Sourisseau, and L. Memery. 2017. Tidal cycle control of biogeochemical and ecological properties of a macrotidal ecosystem. *Geophysical Research Letters* 44 (16): 8453–8462.
- Capriulo, G.M., G. Smith, R. Troy, G.H. Wikfors, J. Pellet, and C. Yarish. 2002. The planktonic food web structure of a temperate zone estuary, and its alteration due to eutrophication. *Hydrobiologia* 475 (476): 263–333.
- Carpenter, E.J., and S. Dunham. 1985. Nitrogenous nutrient uptake, primary production, and species composition of phytoplankton in the Carmans River estuary, Long Island, New York. *Limnology and Oceanography* 30 (3): 513–526.
- Childers, D.L. 1994. Fifteen years of marsh flumes: A review of marsh-water column interactions in Southeastern USA estuaries. In *Global Wetlands: Old World and New*, ed. W.J. Mitsch, 277–294. New York: Elsevier Ltd.
- Cloern, J.E. 1991. Tidal stirring and phytoplankton bloom dynamics in an estuary. *Journal of Marine Research* 49 (1): 203–221.
- Cloern, J.E., S.Q. Foster, and A.E. Kleckner. 2014. Phytoplankton primary production in the world's estuarine-coastal ecosystems. *Biogeosciences* 11 (9): 2477–2501.
- Collos, Y., C. Gagne, M. Laabir, A. Vaquer, P. Cecchi, and P. Souchu. 2004. Nitrogenous nutrition of *Alexandrium catanella* (Dinophyceae) in cultures and in Thau Lagoon, Southern France. *Journal of Phycology* 40 (1): 96–103.
- Davidson, K., R.J. Gowen, P. Tett, E. Bresnan, P.J. Harrison, A. McKinney, S. Milligan, D.K. Mills, J. Silke, and A. Crooks. 2012. Harmful algal blooms: How strong is the evidence that nutrient ratios and forms influence their occurrence? *Estuarine, Coastal and Shelf Science* 115: 399–413.
- Deegan, L.A., and R.H. Garritt. 1997. Evidence for spatial variability in estuarine food webs. *Marine Ecology Progress Series* 147: 31–47.
- Deegan, L.A., J.L. Bowen, D. Drake, J.W. Fleeger, C.T. Friedrichs, K.A. Galván, J.E. Hobbie, C. Hopkinson, D.S. Johnson, J.M. Johnson, L.E. LeMay, E. Miller, B.J. Peterson, C. Picard, S. Sheldon, M. Sutherland, J. Vallino, and R.S. Warren. 2007. Susceptibility of salt marshes to nutrient enrichment and predator removal. *Ecological Applications* 17 (sp5): S42–S63.

- Dortch, Q. 1990. The interaction between ammonium and nitrate uptake in phytoplankton. *Marine Ecology Progress Series* 61: 183–201.
- Drake, D.C., B.J. Peterson, K.A. Galván, L.A. Deegan, C. Hopkinson, J.M. Johnson, K. Koop-Jakobsen, L.E. LeMay, and C. Picard. 2009. Salt marsh ecosystem biogeochemical responses to nutrient enrichment: A paired ¹⁵N tracer study. *Ecology* 90 (9): 2535–2546.
- Duernberger, K., C. Tobias, and M.A. Mallin. 2011. Tracing nitrogen transformations through the food chain in an urbanized tidal creek. Water Resources Research Institute, University of North Carolina, Report 405.
- Dugdale, R.C., F.P. Wilkerson, V.E. Hogue, and A. Marchi. 2007. The role of ammonium and nitrate in spring bloom development in San Francisco Bay. *Estuarine, Coastal and Shelf Science* 73 (1-2): 17–29.
- Fauchot, J., M. Levasseur, and S. Roy. 2005. Daytime and nighttime vertical migrations of *Alexandrium tamarense* in the St. Lawrence Estuary (Canada). *Marine Ecology Progress Series* 296: 241–250.
- Fouilland, E., M. Gosselin, R.B. Rivkin, C. Vasseur, and B. Mostajir. 2007. Nitrogen uptake by heterotrophic bacteria and phytoplankton in Arctic surface waters. *Journal of Plankton Research* 29 (4): 369– 376.
- Giblin, A., C. Tobias, B. Song, N. Weston, G.T. Banta, and V.H. Rivera-Monroy. 2013. The importance of dissimilatory nitrate reduction to ammonium (DNRA) in the nitrogen cycle of coastal ecosystems. *Oceanography* 26 (3): 124–131.
- Glibert, P.M. 2016. Margalef revisited: A new phytoplankton mandala incorporating twelve dimensions, including nutritional physiology. *Harmful Algae* 55: 25–30.
- Glibert, P.M., F.P. Wilkerson, R.C. Dugdale, J.A. Raven, C.L. Dupont, P.R. Leavitt, A.E. Parker, J.M. Burkholder, and T.M. Kana. 2016. Pluses and minuses of ammonium and nitrate uptake and assimilation by phytoplankton and implications for productivity and community composition, with emphasis on nitrogen-enriched conditions. *Limnology and Oceanography* 61 (1): 165–197.
- Harrison, W.G., and L.J.E. Wood. 1988. Inorganic nitrogen uptake by marine picoplankton: Evidence for size partitioning. *Limnology and Oceanography* 33 (3): 468–475.
- Hattenrath, T.K., D.M. Anderson, and C.J. Gobler. 2010. The influence of anthropogenic nitrogen loading and meteorological conditions in the dynamics and toxicity of Alexandrium fundyense blooms in a New York (USA) estuary. *Harmful Algae* 9 (4): 402–412.
- Holmboe, N., H.S. Jensen, and F.Ø. Andersen. 1999. Nutrient addition bioassays as indicators of nutrient limitation of phytoplankton in an eutrophic estuary. *Marine Ecology Progress Series* 186: 95–104.
- Holmes, R.M., J.W. McClelland, D.M. Sigman, B. Fry, and B.J. Peterson. 1998. Measuring ¹⁵N-NH₄⁺ in marine, estuarine and fresh waters: An adaptation of the ammonia diffusion method for samples with low ammonium concentrations. *Marine Chemistry* 60 (3-4): 235–243.
- Holmes, R.M., B.J. Peterson, L.A. Deegan, J.E. Hughes, and B. Fry. 2000. Nitrogen biogeochemistry in the oligohaline zone of a New England estuary. *Ecology* 81 (2): 416–432.
- Hopkinson, C.S., Jr., A.E. Giblin, R.H. Garritt, J. Tucker, and M.A.J. Hullar. 1998. Influence of the benthos on growth of planktonic estuarine bacteria. *Aquatic Microbial Ecology* 16: 109–118.
- Howarth, R.W., G. Billen, D. Swaney, A. Townsend, N. Jaworski, K. Lajtha, J.A. Downing, R. Elmgren, N. Caraco, T. Jordan, F. Berendse, J. Freney, V. Kudeyarov, P. Murdoch, and Z. Zhao-Liang. 1996. Regional nitrogen budgets and riverine N & P fluxes for the drainages to the North Atlantic Ocean: Natural and human influences. *Biogeochemistry* 35 (1): 75–139.
- Hughes, J.E., L.A. Deegan, B.J. Peterson, and R.M. Holmes. 2000. Nitrogen flow through the food web in the oligohaline zone of a New England estuary. *Ecology* 81 (2): 433–452.



- Hunter, B.L., and E.A. Laws. 1981. ATP and chlorophyll *a* as estimators of phytoplankton carbon biomass. *Limnology and Oceanography* 26 (5): 944–956.
- Jeong, H.J., Y.D. Yoo, J.S. Kim, K.A. Seong, N.S. Kang, and T.H. Kim. 2010. Growth, feeding and ecological roles of the mixotrophic and heterotrophic dinoflagellates in marine planktonic food webs. *Ocean Science Journal* 45 (2): 65–91.
- Johnson, K., and R.L. Petty. 1982. Determination of phosphate in seawater by flow injection analysis with injection of reagent. *Analytical Chemistry* 54 (7): 1185–1187.
- Johnson, K., and R.L. Petty. 1983. Determination of nitrate and nitrite in seawater by flow injection analysis. *Limnology and Oceanography* 28 (6): 1260–1266.
- Koch, F., and C.J. Gobler. 2009. The effects of tidal export from salt marsh ditches on estuarine water quality and plankton communities. *Estuaries and Coasts* 32 (2): 261–275.
- L'Helguen, S., J.-F. Maguer, and J. Caradec. 2008. Inhibition kinetics of nitrate uptake by ammonium in size-fractionated oceanic phytoplankton communities: Implications for new production and f-ratio estimates. Journal of Plankton Research 30 (10): 1179–1188.
- Legendre, P. 2018. lmodel2: Model II Regression. R package version 1.7-3. https://CRAN.R-project.org/package=lmodel2. Accessed 1 Dec 2020.
- Leles, S.G., C.A. de Souza, C.O. Faria, A.B. Ramos, A.M. Fernandes, and G.A.O. Moser. 2014. Short-term phytoplankton dynamics in response to tidal stirring in a tropical estuary (Southeastern Brazil). *Brazilian Journal of Oceanography* 62 (4): 341–349.
- Leong, S.C.Y., A. Murata, Y. Nagashima, and S. Taguchi. 2004. Variability in toxicity of the dinoflagellate *Alexandrium tamarense* in response to different nitrogen sources and concentrations. *Toxicon* 43 (4): 407–415.
- Li, W.K.W., R.A. Anderson, D.J. Gifford, L.S. Incze, J.L. Martin, C.H. Pilskaln, J.N. Rooney-Varga, M.E. Sieracki, W.H. Wilson, and N.H. Wolff. 2011. Planktonic microbes in the Gulf of Maine area. *PLoS One* 6 (6): e20981. https://doi.org/10.1371/journal.pone.0020981.
- Lomas, L.M., and P.M. Glibert. 2003. Comparisons of nitrate uptake, storage, and reduction in marine diatoms and flagellates. *Journal* of *Phycology* 36: 903–913.
- Maguer, J.-F., S. L'Helguen, and C. Madec. 2007. Nitrogen uptake and assimilation kinetics in *Alexandrium minutum* (Dinophyceae): Effect of N-limited growth rate on nitrate and ammonium interactions. *Journal of Phycology* 43 (2): 295–303.
- Maguer, J.-F., S. L'Helguen, M. Waeles, P. Morin, R. Riso, and J. Caradec. 2009. Size-fractionated phytoplankton biomass and nitrogen uptake in response to high nutrient load in the North Biscay Bay in spring. *Continental Shelf Research* 29 (8): 1103–1110.
- Margalef, R. 1978. Life-forms of phytoplankton as survival alternatives in an unstable environment. *Oceanologica Acta* 1: 493–509.
- Menden-Deuer, S., and E.J. Lessard. 2000. Carbon to volume relationships for dinoflagellates, diatoms, and other protist plankton. *Limnology and Oceanography* 45 (3): 569–579.
- Moschonas, G., R.J. Gowen, R.F. Paterson, E. Mitchell, B.M. Stewart, S. McNeill, P.M. Glibert, and K. Davidson. 2017. Nitrogen dynamics and phytoplankton community structure: The role of organic nutrients. *Biogeochemistry* 134 (1-2): 125–145.
- Nelson, J.A., L. Deegan, and R. Garritt. 2015. Drivers of spatial and temporal variability in estuarine food webs. *Marine Ecology Progress Series* 533: 67–77.
- Pedersen, M.F., and J. Borum. 1996. Nutrient control of algal growth in estuarine waters. Nutrient limitation and the importance of nitrogen requirements and nitrogen storage among phytoplankton and species of macroalgae. Marine Ecology Progress Series 142: 261–272.
- Peterson, B.J., and B. Fry. 1987. Stable isotopes in ecosystem studies. Annual Review of Ecology and Systematics 18 (1): 293–320.

- pie-lter.ecosystems.mbl.edu. 2018. Plum Island Ecosystems LTER. https://pie-lter.ecosystems.mbl.edu/welcome-plum-island-ecosystems-lter. Accessed August 30, 2018.
- Probyn, T.A., and S.J. Painting. 1985. Nitrogen uptake by size-fractionated phytoplankton populations in Antarctic surface waters. *Limnology and Oceanography* 30 (6): 1327–1332.
- Probyn, T.A., H.N. Waldron, and A.G. James. 1990. Size-fractionated measurements of nitrogen uptake in aged upwelled waters: Implications for pelagic food webs. *Limnology and Oceanography* 35 (1): 202–210.
- R Core Team. 2020. R: A language and environment for statistical computing. R Foundation for Statistical Computing, Vienna. https://www.R-project.org/. Accessed 1 Dec 2020.
- Rabalais, N.N. 2002. Nitrogen in aquatic ecosystems. *Ambio* 31 (2): 102–112
- Ralston, D.K., M.L. Brosnahan, S.E. Fox, K.D. Lee, and D.M. Anderson. 2015. Temperature and residence time controls on an estuarine harmful algal bloom: Modeling hydrodynamics and *Alexandrium* fundyense in Nauset Estuary. Estuaries and Coasts 38 (6): 2240– 2258.
- Redfield, A.C. 1958. The biological control of chemical factors in the environment. *American Scientist* 46: 205–221.
- Sathyendranath, S., V. Stuart, A. Nair, K. Oka, T. Nakane, H. Bouman, M.-H. Forget, H. Maass, and T. Platt. 2009. Carbon-to-chlorophyll ratio and growth rate of phytoplankton in the sea. *Marine Ecology Progress Series* 383: 73–84.
- Schneider, D. 1976. Determination of ammonia and Kjeldahl nitrogen by indophenol method. Water Resources 10: 31–46.
- Shanks, A.L., and A. McCulloch. 2003. Fortnightly periodicity in the abundance of diatom and dinoflagellate taxa at a coastal study site. *Journal of Experimental Marine Biology and Ecology* 296 (1): 113– 126.
- Sigman, D.M., M.A. Altabet, R.H. Michener, D. McCorkle, B. Fry, and R.M. Holmes. 1997. Natural abundance-level measurements of the nitrogen isotopic composition of oceanic nitrate: An adaptation of the ammonium diffusion method. *Marine Chemistry* 57 (3-4): 227– 242.
- Sigman, D.M., K.L. Karsh, and K.L. Casciotti. 2009. Nitrogen isotopes in the ocean. In *The Encyclopedia of Ocean Sciences*, eds. S.A. Thorpe and K.K. Turekian, 2nd ed., 40–54. Elsevier Ltd. https://doi.org/10. 1016/B978-012374473-9.00632-9.
- Spivak, A.C., and J. Ossolinski. 2016. Limited effects of nutrient enrichment on bacterial carbon sources in salt marsh tidal creek sediments. *Marine Ecology Progress Series* 544: 107–130.
- Stauffer, B.A., G.S. Sukhatme, and D.A. Caron. 2020. Physical and Biogeochemical Factors Driving Spatially Heterogeneous Phytoplankton Blooms in Nearshore Waters of Santa Monica Bay, USA. *Estuaries and Coasts* 43 (4): 909–926.
- Stolte, W., and R. Riegman. 1995. Effect of phytoplankton cell size on transient-state nitrate and ammonium uptake kinetics. *Microbiology* 141 (5): 1221–1229.
- Stolte, W., T. McCollin, A.A.M. Noordeloos, and R. Riegman. 1994. Effect of nitrogen source on the size distribution within marine phytoplankton populations. *Journal of Experimental Marine Biology and Ecology* 184 (1): 83–97.
- Strickland, J.D.H., and T.R. Parsons. 1972. A Practical Handbook of Seawater Analysis. 2nd ed, 167. Ottawa: Fisheries Research Board of Canada Bulletin.
- Tada, K., M. Suksomjit, K. Ichimi, Y. Funaki, S. Montani, M. Yamada, and P.J. Harrison. 2009. Diatoms grow faster using ammonium in rapidly flushed eutrophic Dokai Bay, Japan. *Journal of Oceanography* 65 (6): 885–891.
- Teixeira, I.G., B.G. Crespo, T.G. Nielsen, and F.G. Figueiras. 2014. Stratification-mixing cycles and plankton dynamics in a shallow estuary (Limfjord, Denmark). *Journal of Plankton Research* 36 (2): 475–489.



- Terrado, R., A.L. Pasulka, A.A.-Y. Lie, V.J. Orphan, K.B. Heidelberg, and D.A. Caron. 2017. Autotrophic and heterotrophic acquisition of carbon and nitrogen by a mixotrophic chrysophyte established through stable isotope analysis. *The ISME Journal* 11 (9): 2022– 2034.
- Thomas, A.C., D.W. Townsend, and R. Weatherbee. 2003. Satellite-measured phytoplankton variability in the Gulf of Maine. *Continental Shelf Research* 23 (10): 971–989.
- Tobias, C.R., M. Cieri, B.J. Peterson, L.A. Deegan, J. Vallino, and J. Hughes. 2003a. Processing watershed-derived nitrogen in a well-flushed New England estuary. *Limnology and Oceanography* 48 (5): 1766–1778.
- Tobias, C.R., A. Giblin, J. McClelland, J. Tucker, and B. Peterson. 2003b. Sediment DIN fluxes and preferential recycling of benthic microalgal nitrogen in a shallow macrotidal estuary. *Marine Ecology Progress Series* 257: 25–36.
- Underwood, G., and L. Provot. 2000. Determining the environmental preferences of four estuarine epipelic diatom taxa: growth across a range of salinity, nitrate and ammonium conditions. *European Journal of Phycology* 35 (2): 173–182.
- Utermöhl, H. 1958. Zur Vervollkommnung der quantitativen Phytoplankton-Methodik. *Mitteilungen Internationale Verinigung Theoretische und Angewandte Limnologie* 9: 1–38.
- Vallino, J.J., and C.S. Hopkinson Jr. 1998. Estimation of dispersion and characteristic mixing times in Plum Island Sound Estuary. *Estuarine, Coastal and Shelf Science* 46 (3): 333–350.
- Verity, P.G., C.Y. Robertson, C.R. Tronzo, M.G. Andrews, J.R. Nelson, and M.E. Sieracki. 1992. Relationships between cell volume and the

- carbon and nitrogen content of marine photosynthetic nanoplankton. *Limnology and Oceanography* 37 (7): 1434–1446.
- Vörösmarty, C.J., and T.C. Loder III. 1994. Spring-neap tidal contrasts and nutrient dynamics in a marsh-dominated estuary. *Estuaries* 17 (3): 537–551.
- Wafar, M., S. L'Helguen, V. Raikar, J.F. Maguer, and P. Le Corre. 2004. Nitrogen uptake by size-fractionated plankton in permanently well-mixed temperate coastal waters. *Journal of Plankton Research* 26 (10): 1207–1218.
- Weston, N.B., A.E. Giblin, and G.T. Banta. 2010. The effects of varying salinity on ammonium exchange in estuarine sediments of the Parker River, Massachusetts. *Estuaries and Coasts* 33 (4): 985–1003
- Wetz, M.S., K.C. Hayes, A.J. Lewitus, J.L. Wolny, and D.L. White. 2006. Variability in phytoplankton pigment biomass and taxonomic composition over tidal cycles in a salt marsh estuary. *Marine Ecology Progress Series* 320: 109–120.
- Xu, J., P.M. Glibert, H. Liu, K. Yin, X. Yuan, M. Chen, and P.J. Harrison. 2012. Nitrogen sources and rates of phytoplankton uptake in different regions of Hong Kong waters in summer. *Estuaries and Coasts* 35 (2): 550–571
- York, J.K., G. Tomasky, I. Valiela, and D.J. Repeta. 2007. Stable isotopic detection of ammonium and nitrate assimilation by phytoplankton in the Waquoit Bay estuarine system. *Limnology and Oceanography* 52 (1): 144–155.
- Zobell, C.E. 1943. The effect of solid surfaces upon bacterial activity. *Journal of Bacteriology* 46 (1): 39–56.

